原子配列が制御された多孔性電極による水素生成反応の効率化
Electrochemical hydrogen evolution reaction using porous nanostructured electrode with controlled atomic surface structure

研究代表者　国立研究開発法人産業技術総合研究所　研究グループ長　三重 安弘
Yasuhiro Mie, Group leader, National Institute of Advanced Industrial Science and Technology (AIST)

1. Introduction

Due to global environmental issues, there has been a strong demand for the development of sustainable technology in many fields. Bearing this in mind, electrocatalysis with an electrode is a promising approach in chemical production because it can efficiently utilize electricity from renewable energy [1]. As the hydrogen molecule is a viable energy source, efficient electrochemical hydrogen evolution at an electrode catalyst is expected be a crucial factor in developing a hydrogen economy. In electrochemical methods, an electrode works as a catalyst and an electron server/receiver. Therefore, in addition to the nature of the electrode materials, its surface structure is a key factor that determines the catalytic activity. Owing to the growth of nanotechnological methods, electrodes composed of nanomaterials and the nanostructurization of electrode surfaces have been developed [2]. Now, it is well-recognized that the nanoarchitecture of electrodes significantly enhances the electrocatalytic activity, and one of the reasons is the abundant low-coordinated surface atoms at the steps/kinks [3]. Among many types of nanostructured electrodes, nanoporous metals have been attracted in many fields owing to their large surface area [4]. Nanoporous gold (NPG) is promising in electrochemical applications of catalysis and sensing, owing to its advantages, such as high conductivity, catalytic activity, chemical inertness, physical stability, reusability, and facile surface modification. Besides nanostructure effect, the surface atomic structure (crystallographic orientation) of the electrode catalyst plays a crucial role in determining the activity for electrochemical reactions. Fairly recently, we have developed a facile method to prepare NPG and its surface atomic structure can be controlled by changing the conditions in preparation procedure [5].

Currently, it is recognized that Pt-based materials catalyze the HER most efficiently. However, the scarcity of Pt limits its use and requires to develop another electrode catalyst for HER. Although gold material is stable and can be useful electrode catalyst, its HER activity is very poor (Fig. 1). In the present study, we prepared NPG electrode

with different atomic surface structure, and examined their HER activity, aiming the improvement in efficiency of electrochemical HER.

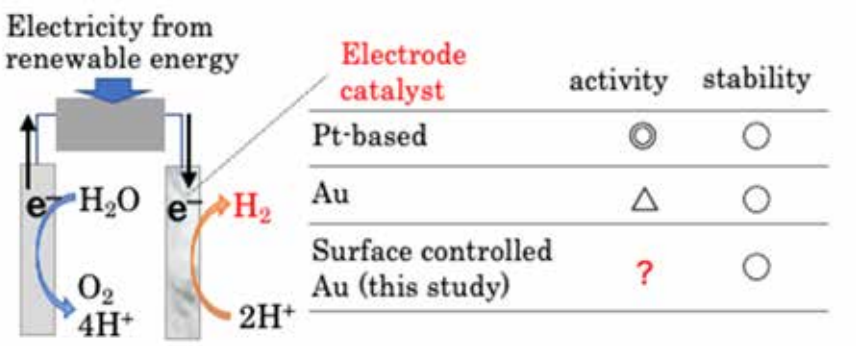

Fig. 1. Electrochemical hydrogen evolution reaction (HER) and comparison of the catalysts for the hydrogen production.

2. Experimental

Electrochemical measurements were mostly performed with a normal three-electrode configuration consisting of an Ag|AgCl|sat.KCl reference electrode, a Pt auxiliary electrode, and a gold electrode.

Anodization was used to prepare nanoporous structure on the gold electrode catalyst according to our previous reports [5]. NPGs with different atomic surface structures were obtained by changing the electrolyte solution in the anodization process. The surface morphology and crystallographic orientation were analyzed using scanning electron microscopy (SEM) and cyclic voltammetry discussed below, respectively.

Gold nanoparticles (AuNPs) were also used to produce nano(porous) structured electrode surface. Solution plasma method was conducted to prepare 10-20 nm sizes of AuNPs [6].

3. Results and Discussions

3.1 HER at anodized NPG with different surface atomic structure

Anodization of commercially available gold electrode produced nanoporous structure as shown in Fig. 2a,b, composed of ligaments and pores. The morphology of NPG obtained under different electrolyte condition (35 and 500 mM chloride ion) was similar, and that of gold electrode surface before anodization process exhibited the planar surface (Fig. 2c).

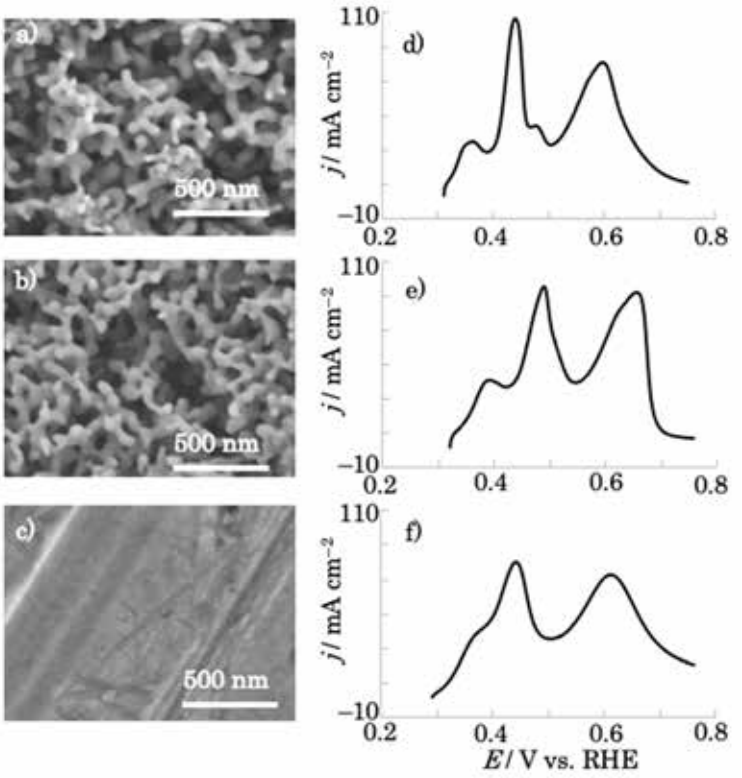

Fig. 2. (a–c) Surface morphology by SEM and (d–f) Pb-UPD-stripping voltammograms of (a, d) NPG-35, (b, e) NPG-500, and (c, f) normal gold.

While having the similar morphologies, the voltammetric responses in the presence of Pb^{2+} (Pb underpotential deposition (UPD) and stripping properties) differed significantly between the aforementioned NPGs, as shown in Fig. 2d,e. Pb-UPD and stripping measurements are generally used to evaluate the crystallographic orientations (atomic structure) of gold electrode surfaces. NPG prepared from the solution containing 35 mM Cl^- (NPG-35) exhibited main anodic peaks at 0.444 and at approximately 0.600 V (Fig. 2d). The former was sharp and close to the potentials of the stripping of Pb on Au(111). On the other hand, NPG prepared from the solution containing 500 mM Cl^- (NPG-500) exhibited anodic currents at 0.492 and around 0.660 V with a shoulder peak at 0.622 V. The former peak was close to that representing Pb stripping on the Au(100) surface. The voltammogram of the normal planar (before anodization) gold electrode showed two broad stripping peaks around 0.444 and 0.610 V shown in Fig. 2f. These differences in peak positions for each surface indicate that the NPGs and normal gold surfaces have different facet contributions. We also confirmed a considerable amount of Au(111) and Au(100) facets in NPG-35 and NPG-500, respectively, by electrochemical reductive desorption peaks of self-assembled monolayer film on these gold surfaces. All results indicate that the normal, NPG-35, and NPG-500

have Au(110)-, Au(111)-, and Au(100)-rich surfaces, respectively.

Since the NPG electrodes having different facet contributions were confirmed, then we examined the electrochemical HER with these NPG electrodes to investigate the effect of the surface atomic structure of nanostructured catalyst on the reaction. Fig. 3A represents the obtained voltammograms at NPGs in a 0.5 M H_2SO_4 solution with iR compensation in comparison with that of normal gold electrode, where the current density, j, in mA cm^{-2}, was calculated from the actual surface area estimated electrochemically from the reductive charge of AuO. As shown in Fig. 3A, NPG-35 exhibited a larger catalytic current than NPG-500 and normal gold. The current density in the voltammogram obtained for NPG-35 was more than 2 and 15 times larger than those for NPG-500 and normal gold, respectively, at –0.1 V. The potentials providing the current density of 3 mA cm^{-2} were –0.048 V for NPG-35, whereas those of NPG-500 and normal gold were –0.073 and –0.149 V, respectively. The overpotential value for the NPG-35 electrode was considerably lower compared with those of other gold-based catalysts [7], indicating the effective enhancement in the hydrogen production by the present nanostructurization. Because NPG-35 and NPG-500 have similar morphologies when they have similar electrochemical surface areas, as shown in Fig. 2, the difference in current density for the HER may be ascribed to the difference in the facet compositions of each surface. Previous report, which used single-crystal gold electrode, showed that Au(111) exhibited about 2.3 times larger catalytic current than Au(100) [8]. Further, gold nanospikes electrode having Au(111) dominated surface is also reported to show significant increase in the current density for HER [9]. Our results are consistent with these phenomena.

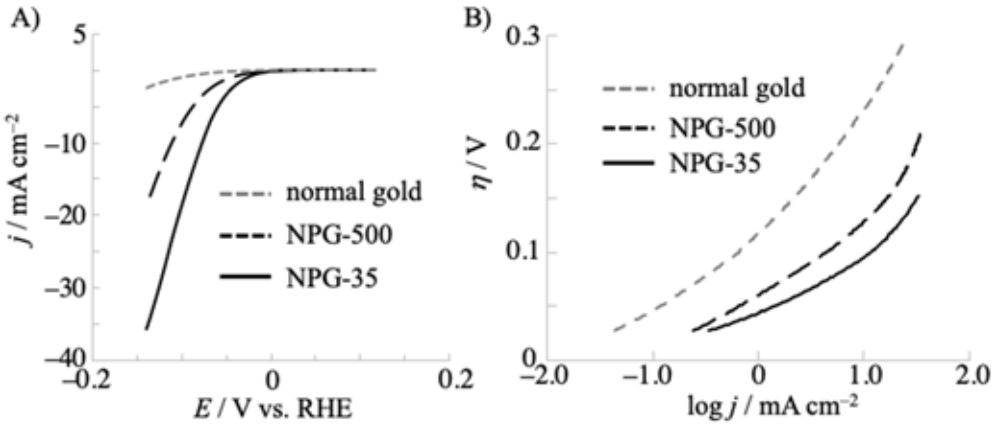

Fig. 3. (A) Polarization curves obtained at NPGs and normal gold electrodes in 0.5 M H_2SO_4 and (B) the corresponding Tafel plots.

Fig. 3B represents the Tafel plot for further understanding of the reaction [10]. The slopes of both NPGs and normal gold varied between lower and higher overpotential regions, similar to those in previous reports for gold-based catalysts [10,11]. The slopes for normal gold were 69 and 150 mV dec^{-1} in the lower and higher overpotential regions, respectively. These values are within the reported region for gold-based catalysts, indicating that the formation of a surface-adsorbed hydrogen atom (the proton discharge reaction known as the Volmer reaction) is the rate-determining step. The NPG-35 and NPG-500 exhibited the slopes of 42 and 57 mV dec^{-1} in the lower region, and 118 and 170 mV dec^{-1} in the higher region, respectively. The decrease of the slope in the lower region indicates the enhanced H adsorption process on the NPG surface owing to the nanostructured effect. The slope variation for NPG-35 is close to those of the simulated curve (40 and 120 mV dec^{-1} in the lower and higher overpotential regions, respectively); here, an electrochemical desorption reaction (Heyrovsky reaction) is the rate-determining step, indicating the HER occurs through Volmer-Heyrovsky mechanism at NPG-35. These observation reveals the importance of the control of the crystallographic orientation in nanostructured catalysts in electrocatalytic reactions. Thus, the obtained outcomes clearly demonstrate that the preparation of NPG utilizing the present method is remarkably effective for the development of efficient catalysts.

3.2 HER at AuNP deposited nano(porous)structured electrode

The HER was also investigated using AuNPs deposited thin film electrode with a certain atomic surface structure. AuNPs used in this study mostly had diameters between 10 and 20 nm, as shown in the Transmission Electron Microscopy (TEM) image (Fig. 4a). The concentrated aqueous solution with around 0.2 wt% dispersed AuNPs was dropped on the GC electrode surface and left under air to evaporate the remaining aqueous solution. The drying process finished within 48 h. A AuNP thin film exhibiting a golden metallic color was obtained, as shown in Fig. 4b, with a diameter of 6.0 mm. Fig. 4c and 4d show SEM images of the commercial planar and the AuNP thin film gold surfaces. The AuNP thin film was formed by drying the concentrated aqueous dispersion of AuNPs on the GC surface, so the AuNPs were piled on top of each other. Consequently, the top view of the SEM image shows the true appearance. It has been suggested that there should be nanostructures based on AuNPs inside the AuNP thin film, compared with the commercial planar gold electrode (see Fig. 4c and d). The XRD pattern of a AuNP thin film on a glass substrate prepared using the same method as the present study exhibited four main diffraction peaks corresponding to the (111), (200), (220), and (311) planes of gold metal with 2θ between 30 and 80 degrees (JCPDS, No.

04-0784), revealing the excellent crystallinity of AuNP on the substrate. A similar result was expected for the present AuNP thin film electrode on the GC substrate.

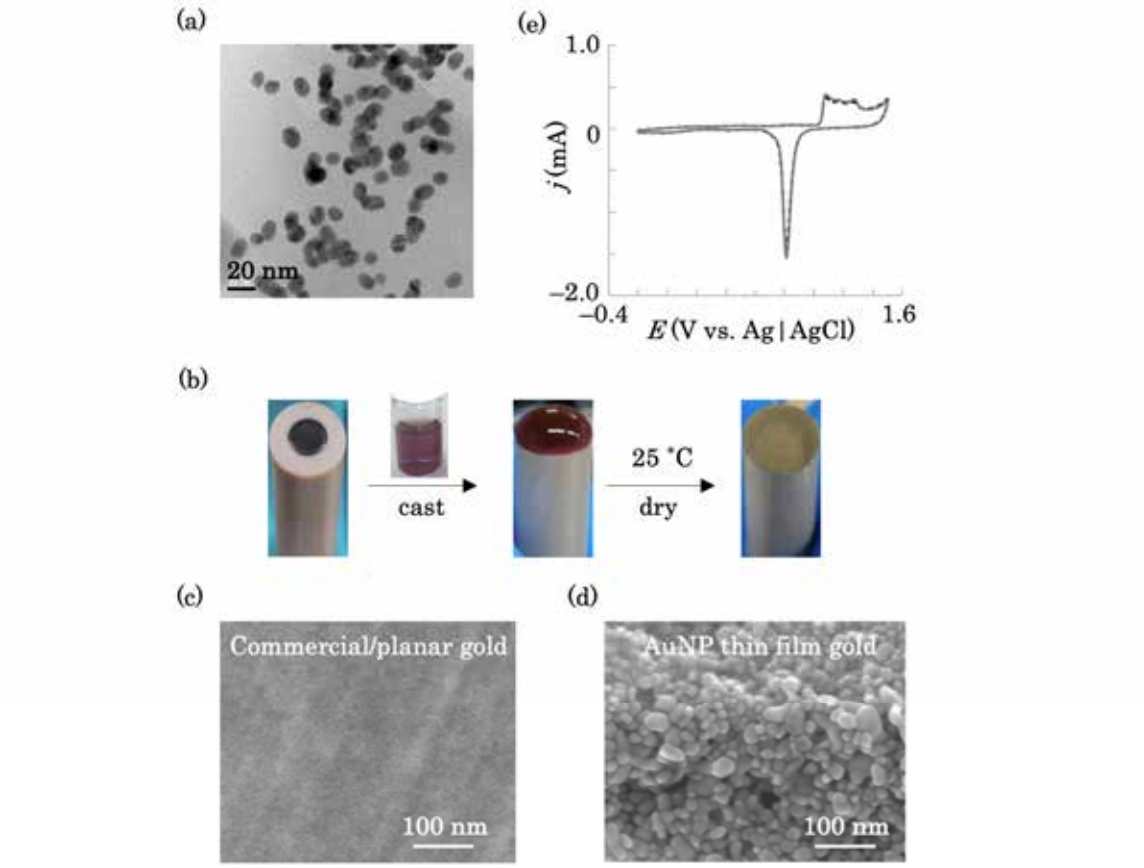

Fig. 4 (a) TEM image of the AuNP dispersed solution used in this study. (b) Schematic representation for the preparation of AuNP thin film electrode on the commercial glassy carbon disk electrode. (c, d) SEM images of the (c) commercial disk and (d) AuNP thin film gold electrode surfaces. (e) Cyclic voltammograms obtained in a 0.5 M H_2SO_4 solution at AuNP thin gold film electrode before (dashed line) and after (solid line) 200 cycles/measurements.

The AuNP thin film produced the typical cyclic voltammograms of a gold electrode in H_2SO_4 solution, as shown in Fig. 4e. The peak currents are clearly recognizable, originating from surface oxide formation and their reduction. The surface area of the film electrode prepared from the 2 mg/mL AuNPs solution was estimated from the reductive charge of the surface oxide film in the voltammogram to be 2.4 cm^2, giving a surface roughness of 8.6 using the geometric area of the electrode with a diameter of 6 mm. Importantly, the voltammograms in a 0.5 M H_2SO_4 solution were almost unchanged after 200 cycles (measurements), although no binder was used for the AuNP/GC disk. This showed that the AuNP thin film electrode exhibited a stable electrochemical response (dotted and solid lines in Fig. 4e). We also confirmed that the AuNP thin film electrode prepared on GC is stable when stored at room temperature

for more than 1 year [12].

Fig. 5a shows the linear sweep voltammograms recorded in a 0.5 M H_2SO_4 solution at AuNP thin film and planar gold electrodes. The currents are represented by the current density using the actual/electrochemical electrode surface area estimated electrochemically from the reductive charge of the surface AuO of these gold electrodes. It can be clearly seen that the AuNP thin film electrode exhibited a much higher catalytic current than the planar gold electrode. The current density of 27 mA cm^{-2} in the voltammogram obtained at the AuNP thin film electrode was more than 10 times larger than that at the planar gold electrode at −0.13 V vs RHE, and was close to that (30 mA cm^{-2}) reported for nanoporous gold electrodes prepared by an anodization technique [5]. The potential providing the current density of 3 mA cm^{-2} was −0.094 and −0.194 V for the AuNP thin film and commercial gold electrodes, respectively. The overpotential value obtained at the AuNP thin film electrode was considerably lower than those of planar and other gold-based catalysts similar to the previous case. These results indicate that electrode surface nanostructuring by reagent-free AuNPs effectively enhanced the electrochemical activity towards HER. Perez et al. studied HER with gold single-crystal electrodes. They suggested that the activity for HER increases on Au(111) > Au(100) > Au(110) planes [8], highlighting the significance of the

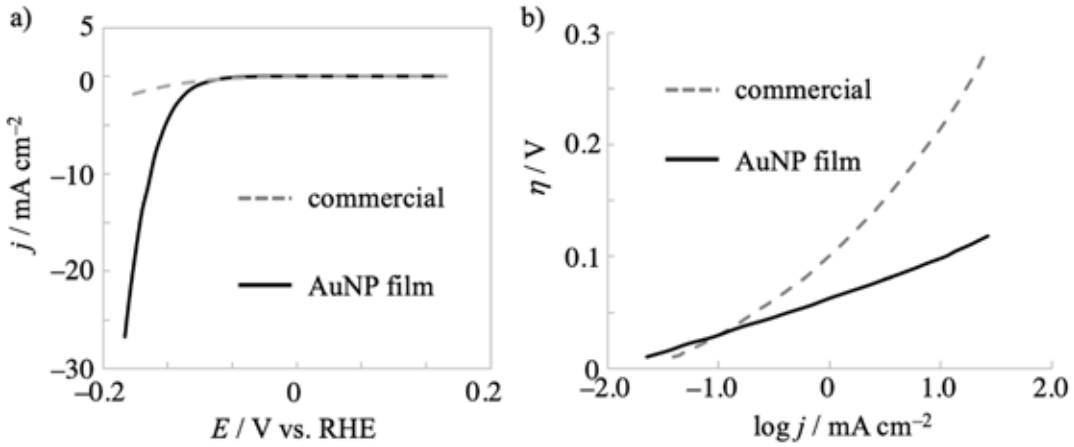

Fig. 5. (a) Linear sweep voltammograms for hydrogen evolution reaction obtained at AuNP thin film (solid line) and commercial disk (dashed line) gold electrodes at a scan rate of 2 mV s^{-1} in a 0.5 M H_2SO_4 and (b) the corresponding Tafel plots.

surface atomic structure for this reaction. We compared the voltammetric features of planar and AuNP thin film gold electrodes to obtain information on the crystal planes. Compared with the planar gold electrode, the AuNP thin film exhibits increased oxidation peaks at 1.1 and 1.3 V, which correspond to Au(100) and Au(111) planes, respectively. Therefore, the enhanced (111) and the surface of the present AuNP film

gold electrode may improve HER performance.

A Tafel analysis was conducted to further understand the HER reaction at the AuNP thin film electrode. The Tafel plot is shown in Fig. 5b, together with the results for the planar gold electrode. The slope obtained for planar gold in the higher overpotential region was 134 mV dec^{-1}. This value is within the reported range measured at gold-based electrodes. This indicates that the proton discharge reaction (the formation of a surface-adsorbed hydrogen atom), known as the Volmer reaction, determined the rate. By contrast, the AuNP thin film electrode exhibited a slope of 39 mV dec^{-1}. The lower slope indicates a faster H adsorption process on the AuNP thin film electrode surface. The value of the slope suggests that the electrochemical desorption reaction (known as the Heyrovsky reaction) was the rate determining step. Hence, HER is expected to take place through the Volmer–Heyrovsky mechanism at the AuNP thin film electrode. This phenomenon is similar to the aforementioned anodized NPG case. Due to the lower free energy for hydrogen adsorption, the abundant low-coordinated surface atoms at the steps/kinks in the nanostructured surface would cause enhanced H adsorption at the AuNP thin film surface [13]. Thus, the nanostructured and facet effects would enhance HER activity at the present AuNP thin film electrode.

3.3 α-Keto acid reduction at anodized NPG with controlled atomic surface structure

Concomitantly, we also found that the anodized NPG-500 shows improved catalytic activity for α-keto acid reduction to the corresponding amino acid [14]. A reductive voltammetric signal at the NPG electrode appeared at a more positive potential by 0.18–0.79 V, compared with those at the planar-gold electrode without anodization and other previously reported electrode systems (as shown in Fig. 6), indicating the high activity of the prepared nanostructure for the electrochemical reaction. Maximum Faradaic efficiencies (FEs) of 74–93% in the reductive molecular conversion to amino acids of Ala, Asp, Glu, Gly, and Leu were obtained under the optimized conditions. The FE values were strongly dependent on the applied potential in the electrolysis, suggesting that the hydrogen evolution reaction at the electrode surface was more significant as the applied potential became more negative. The effect of potential at the NPG was lower than that at the planar-gold electrode. These results indicate that nanostructurization decreases the overpotential for the electrochemical reductive amination, resulting in high FE.

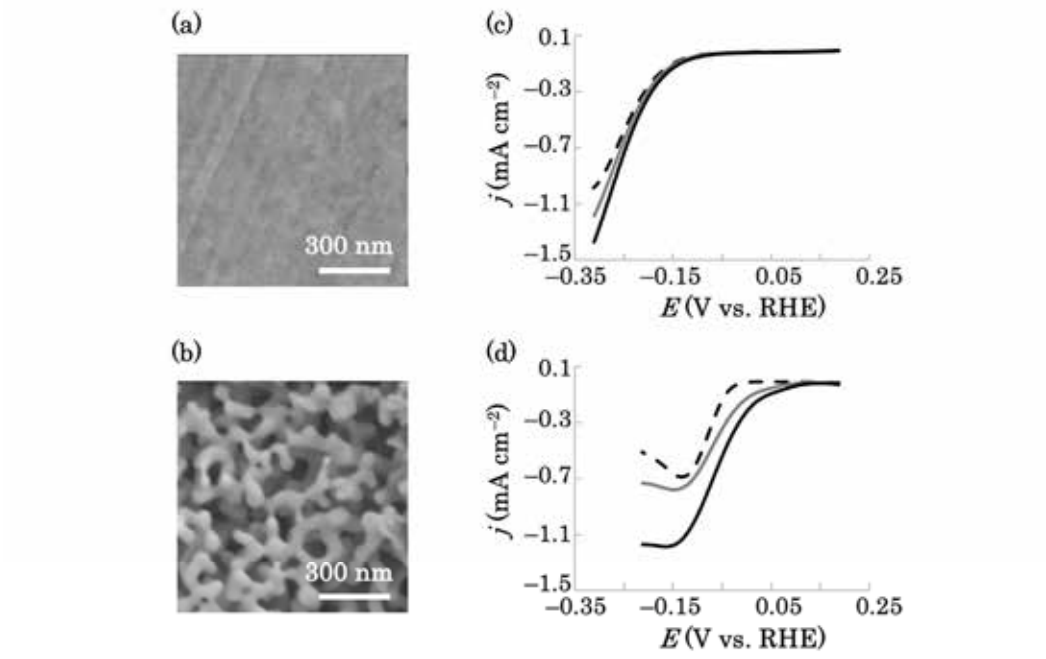

Fig. 6. Surface morphologies of (a) planar (non-anodized) gold and (b) anodized NPG-500 electrodes. Voltammograms obtained for 25 mM (gray line) and 50 mM (black line) α-ketoglutaric acid in 0.15 M NaCl solution containing 50 mM NH_2OH at (c) planar gold and (d) NPG-500 electrodes. Dashed lines indicate voltammograms recorded without α-ketoglutaric acid and NH_2OH.

4. Conclusion

In developing a hydrogen society, efficient electrochemical hydrogen evolution reaction (HER) at an electrode catalyst can be a crucial strategy. Although gold is stable and can be useful electrode catalyst, its HER activity is very poor. In this study, porous nanostructured gold surfaces with controlled atomic surface structures were prepared and their HER activity was investigated. We found that nanostructured gold surface with Au(111)-rich surface showed considerably larger (more than 15 times and 2 times) activity in current density for HER compared with those at polycrystalline planar gold and nanostructured gold with Au(100)-rich surfaces, respectively. On the other hand, electrochemical reductive reaction of α-keto acid to the corresponding amino acid was significantly improved at the nanostructured gold electrode catalyst with Au(100) surface. Results suggest that the present method to control the atomic surface structure of electrode surface is promising to develop efficient electrode catalyst for electrochemical reactions.

Acknowledgement

The author acknowledges the financial supports from JFE 21st Century Foundation.

謝辞

本研究は、公益社団法人 JFE21 世紀財団より技術研究助成の支援を受けて行いました。ここに謝意を表します。

References

1) Wang, F. M.; Li, W. J.; Wang, R.; Guo, T. Q.; Sheng, H. Y.; Fu, H. C.; Stahl, S. S.; Jin, S., *Joule* **2021,** *5*, 149-165.
2) Liang, J.; Liu, Q.; Li, T. S.; Luo, Y. L.; Lu, S. Y.; Shi, X. F.; Zhang, F.; Asiri, A. M.; Sun, X. P., *Green Chem.,* **2021,** *23*, 2834-2867.
3) Biener, J.; Biener, M. M.; Madix, R. J.; Friend, C. M., *Acs Catal.,* **2015,** *5*, 6263-6270.
4) Bhattarai, J. K.; Neupane, D.; Nepal, B.; Mikhaylov, V.; Demchenko, A. V.; Stine, K. J., *Nanomaterials* **2018,** *8*, 171.
5) Mie, Y.; Takayama, H.; Hirano, Y., *J. Catal.* **2020,** *389*, 476-482.
6) Matsuda, N.; Nakashima, T.; Okabe, H.; Yamada, H.; Shiroishi, H.; Nagamura, T., *Mol. Crys. Liq. Crys.,* **2017**, 653, 137-143.
7) Renjith, A.; Roy, A.; Lakshminarayanan, V., *J. Coll. Int. Sci.,* **2014,** *426*, 270-279; Siddhardha, R. S. S.; Lakshminarayanan, V.; Ramamurthy, S. S., *J. Power Sources* **2015,** *288*, 441-450.
8) Perez, J.; Gonzalez, E. R.; Villullas, H. M., *J. Phys. Chem. B* **1998,** *102*, 10931-10935.
9) Plowman, B.; Ippolito, S. J.; Bansal, V.; Sabri, Y. M.; O'Mullane, A. P.; Bhargava, S. K., *Chem. Commun.,* **2009**, 5039-5041.
10) Zou, X. X.; Zhang, Y., *Chem. Soc. Rev.,* **2015,** *44*, 5148-5180.
11) Khanova, L. A.; Krishtalik, L. I., *J. Electroanal. Chem.,* **2011,** *660*, 224-229.
12) Mie, Y.; Okabe, H.; Mikammi, C.; Motomura, T.; Matsuda, N. *Electrochem., Commun.,* **2022**, 146, 107415.
13) Lu, J.; Zhou, W. J.; Wang, L. K.; Jia, J.; Ke, Y. T.; Yang, L. J.; Zhou, K.; Liu, X. J.; Tang, Z. H.; Li, L. G.; Chen, S. W., *Acs Catal.,* **2016,** *6*, 1045-1053.
14) Mie, Y.; Katagai, S.; Mikammi, C. *Int. J. Mol. Scie.,* **2021**, 22, 9442.